

Applying Rough Sets for the Identification of Significant Variables in Photovoltaic Energy Production with Isolated Systems

José Antonio Pérez Rodríguez^a, Florentino Fdez-Riverola^{b,c*}

^aCFR: Centro de Formación e Recursos, Rúa da Universidade s/n, A Cuña Mariñamansa, 32005, Ourense, Spain

^bESEI: Escuela Superior de Ingeniería Informática, Campus Universitario As Lagoas s/n, 32004, Ourense, Spain

^cCITI: Centro de Investigación, Transferencia e Innovación, Parque Tecnológico de Galicia - Tecnópole, Avda. de Galicia Nº 2, San Ciprian das Viñas, 32900, Ourense, Spain

*Corresponding author: riverola@uvigo.es

Article history

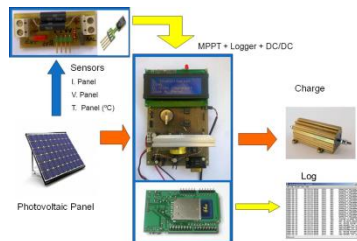
Received :11 September 2012

Received in revised form :

21 February 2013

Accepted :15 April 2013

Graphical abstract



Abstract

The main objective of this work is to study the state of the art of current techniques and algorithms for improving the efficiency of isolated solar photovoltaic systems. Additionally, a study will be conducted regarding the feasibility of applying rough sets (RS) for the practical identification of a minimum set of significant input variables (condition attributes) which determine the value of the output variables (decision attributes) in solar photovoltaic systems. Several experiments were carried out using a TS97 solar photovoltaic system donated by T-Solar for research purposes. The developed system was used to capture the values of input variables in different periods of time and climatic conditions (obtained through a MeteoGalicia monitoring station). The experimental prototype implemented was composed of a solar photovoltaic panel, a resistive load to dissipate the energy generated by the panel, a MPPT (*Maximum Power Point Tracking*) placed between the panel and the charge, a data logger equipped with a RTC (*Real-Time Clock*) and several sensors for measuring the values of physical and electrical variables of the system. Data captured was stored in a 2GB solid state card using a plain text format in order to facilitate later study and analysis using RS.

Keywords: Isolated solar photovoltaic systems; MPPT algorithms; rough sets; variable selection; classification quality

© 2013 Penerbit UTM Press. All rights reserved.

1.0 INTRODUCTION AND MOTIVATION

Nowadays, it is not necessary to point out the relevance of renewable and clean energies (solar, wind, tidal, biomass, etc.), as well as the benefits they are currently bringing and they could bring to our high-tech society in need of energy. Although the worldwide production is still low (less than a 10%), it is remarkable the rise of this type of energies during this century, mainly due to the increasing awareness of environmental respect, and the significant R&D investments of many countries in this field.

Focusing on electrical energy production by photovoltaic systems, Spain is one of the world's leading producers. Specifically, at present, Spain is the second largest producer at a considerable distance from Germany, the largest producer, although solar radiation in Spain is a 20% higher than in Germany.

In Spain, solar power potential is much greater than wind power and, statistically, more predictable and constant. Additionally, installation and maintenance costs of solar power plants by energy power unit produced are much lower. However, solar power is still at the bottom in the renewable energy mix due

to its low *energy efficiency*. This means that energy produced by a solar panel throughout its lifetime (25 to 30 years) is not much greater than the energy needed for its manufacturing.

To address this problem, it is necessary to reduce the manufacturing costs and, especially, to increase the energy efficiency (watt of electricity generated by watt of solar radiation received), as nowadays it is below the 15% in commercial systems. Regarding this issue, MPPT (*Maximum Power Point Tracking*) is one of the most commonly used techniques for increasing the energy efficiency of solar photovoltaic systems [1].

In this context, the most important part of a solar photovoltaic system is the solar photovoltaic panel. This is a device responsible for the direct transformation of solar energy coming from the sun in the form of photons (radiation) into electrical energy, which can be directly injected into the transport grid or stored in batteries for later use. The most common type of solar cells is based on the photovoltaic effect, which stands that light incident on a two-layer semiconductor device (usually silicon) produces a voltage or potential difference between both layers. This voltage is capable of conducting electricity through an external circuit and produce useful work.

A current solar panel can generate a maximum power of a few hundred watts. In order to increase this power, photovoltaic solar panels are linked with serial/parallel connections, allowing the generation of tens of kilowatts or, even, megawatts. Photovoltaic panels are usually oriented towards the sun and, therefore, exposed to a broad range of environmental conditions, such as wind, humidity, atmospheric pressure, rain, etc. Although there are many types of panels, the most commons at present in solar installations can be divided into the following categories:

- (1) *Monocrystalline Silicon Panels*: Made from cylindrical monocrystalline silicon bars (one single crystal). Efficiency between 15% and 18%. Difficult to manufacture and high cost.
- (2) *Polycrystalline Silicon Panels*: Made from silicon block obtained from fusion of pure silicon pieces. Efficiency between 12% and 15%. Difficult to manufacture and high cost, but below monocrystalline.
- (3) *Amorphous Silicon Panels (Thin Film)*: Made by depositing thin layers of silicon on glass or metal substrate. Efficiency

below 10%. Easy to manufacture and low cost. This is the technology selected for the present study.

A photovoltaic system is usually defined as a set of mechanic, electric and electronic components used for harnessing available solar energy and transforming it into electrical energy. Based on their configuration, generated power and installation place, these systems are classified into two different categories: (i) isolated systems (Figure 1), and (ii) grid connection systems (Figure 2).

Isolated systems are commonly used for supplying electricity at distant places, where the geographic location and the limited access make the connection to the conventional electricity grid unprofitable. Due to this fact, isolated systems are usually equipped with storage batteries for storing produced energy. Storage is needed as the photovoltaic system depends on radiation captured during the day, while the user energy demand is usually higher on the evening and night. The cost and maintenance of this type of systems is much higher than in photovoltaic systems connected to the electricity grid

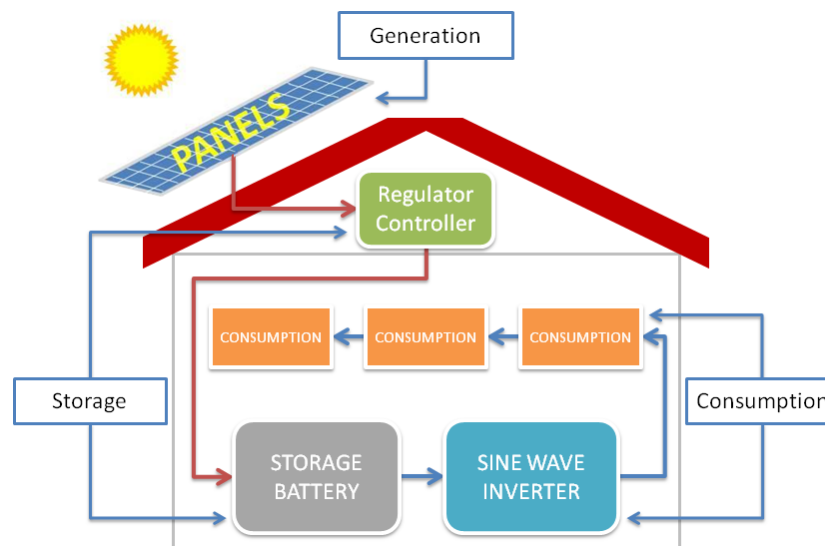


Figure 1 Isolated photovoltaic system

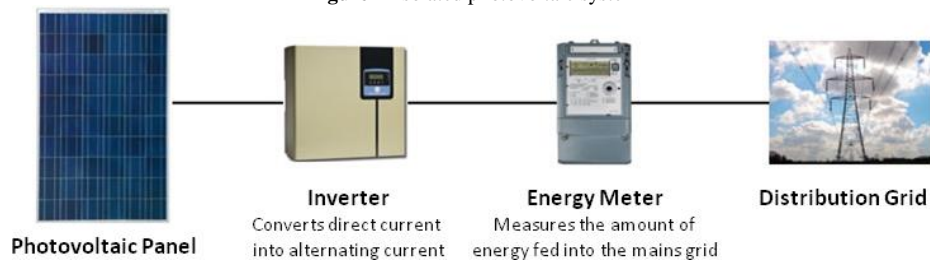


Figure 2 Grid connection photovoltaic system

Grid connection systems, contrary to other isolated systems, do not include storage batteries for the energy generated by the system, because the energy produced during sunshine hours is directly injected into the transport grid [2]. Nowadays, this type of systems is widely used by individuals for selling energy, because of its simplicity, low cost and great subsidies.

In this context, the main objective of the current work is the identification of a minimum set of variables with a high impact on photovoltaic solar energy production at isolated systems (as shown in Figure 1) applying rough set theory [3]. This proposal

is particularly interesting because we expect to increase the system efficiency while reducing the overall system cost, as the sensors used for capturing the aforementioned variables will become unneeded [4].

The rest of the work is structured as follows: Section 2 presents a review of the state of the art of MPPT algorithms. Section 3 details the specific hardware and software implementation required for real data capturing. In Section 4, data sources used in this study are identified, together with the results of applying RS for selecting significant variables and the

discussion about different problems confronted during this research. Finally, Section 5 summarizes the work and establishes some future research lines. Additionally, this work incorporates two appendices in which relevant information about different aspects of the experimentation carried out are outlined.

2.0 MPPT: OPERATION AND COMMON APPROACHES

A solar collector can operate in a wide range of voltage and intensity. This variation can be achieved by changing the load resistance in the electric circuit or modifying the photocell impedance from zero (short circuit value) to high values (open circuit). With regard to this behavior, we can determine the maximum power point defined as the configuration to maximize V and time regarding I (i.e.: the collector optimal load to achieve the maximum electric power from a particular radiation level).

The maximum power point of a solar device varies depending on the incident light. In order to build great solar farms, we can assume an increase in costs introduced by the usage of devices to measure instantaneous power by monitoring voltage and intensity, and therefore use this information to perform real-time and dynamical load adjusts to ensure the transfer of the maximum power regarding changes in lighting conditions happened during the whole day.

Related to this concept, the *maximum point power tracking* (usually known as MPPT) stands for a hybrid electric system (hardware and software) operating between the solar collector and load to aid in the production of the greatest amount of energy by varying the point of electrical operation of solar collectors (Appendix A provides a detailed explanation about their operation). As showed in Table 1, different algorithms are currently used to achieve an adequate tracking of maximum power point [5-7].

Table 1 Common MPPT algorithms

Algorithm	Convergence speed	System complexity
Hill climbing	Variable	Low
Perturb and Observe (P&O)	Variable	Low
Incremental Conductance	Variable	Medium
Neural Networks	High	Very High
Fractional ISC	Medium	Medium/Low
Fractional VOC	Medium	Medium/Low
Fuzzy Logic Control	High	Very High

In general, algorithms included in Table 1 behave in a similar way by analyzing environmental conditions and current value of load or collector. As we can realize from Table 1, the best algorithms to handle both high environmental conditions and load changing situations require the usage of complex algorithms, being classified as *pseudo-MPPT* and *real MPPT* algorithms.

The *pseudo-MPPT* algorithms family is based on the proportionality of voltages in open circuit [8] (V_{oc}) or intensity in short-circuit (I_{sc}) of photovoltaic collector, and voltage (V_{mppt}) or intensity (I_{mppt}) in the maximum power point. These approaches have the disadvantage of requiring to disconnect or short-circuit the collector and load during a short period of time, with the corresponding power loss. Voltage in open circuit and intensity in short-circuit are respectively represented in Equations (1) and (2).

$$V_{mppt} = V_{oc} \times K, \quad K \in [0.72, 0.78] \quad (1)$$

$$I_{mppt} = I_{sc} \times K, \quad K \in [0.78, 0.92] \quad (2)$$

Algorithms included in the *real MPPT* algorithm family are able to continuously track the point of maximum power by oscillating left and right, but they present the drawback of the time required to converge and the curly power curve produced by the converter of the oscillation. The most common algorithms within this category are: *Hill climbing*, *Perturb and Observe (P&O)* [9] and *Incremental conductance*. Due to their special interest, we include in this work a brief description of the most important details concerning their operation [10].

On the one hand, the Hill climbing procedure is able to relate photovoltaic solar collector power and power interface (DC/DC converter) duty cycle (D). The sign of the curve $P = f(\text{Volt. Panel})$ should be analyzed for each sampling point, adjusting the voltage when changing the duty cycle (D).

On the other hand, P&O algorithm compares the values of current and last instantaneous power measurements (P_k and P_{k-1} ,

respectively). The goal of this contrast is to find a voltage or intensity variation as effect of the usage of a constant coefficient to reduce or increase panel variable up to achieve the maximum point of power [11].

Finally, the incremental conductance algorithm (also known as *derivative 0*) is founded on the principle establishing that the slope of the collector power curve is 0 in the maximum power point, being positive on the left side of this point and negative on the right side. Equations (3) to (5) define this behavior.

$$dP/dV = 0 \Rightarrow \text{MPP} \quad (3)$$

$$dP/dV > 0 \Rightarrow \text{left of MPP} \quad (4)$$

$$dP/dV < 0 \Rightarrow \text{right of MPP} \quad (5)$$

Moreover, during the last years new techniques and algorithms based on fuzzy logic and neural networks [12] have been introduced in order to support real MPPT and achieving high speed and confluence precision level. However, these approaches present a large system complexity. Due to this drawback, their application in real environments is limited to great power production stations, being unsuitable to be applied to isolated photovoltaic systems as the target of the present work.

3.0 SPECIFIC HARDWARE AND SOFTWARE IMPLEMENTATION

In order to optimize the amount of energy produced by the photovoltaic solar collector under study (see Appendix B for the specific characteristics) as near of the maximum power point (MPP) as possible and addressing the effects of environmental condition variations, we have designed and built both a specific hardware (data logger) and the complementary firmware for the global control of the system [13]. Figure 3 shows the data capture system implemented to carry out the present study.

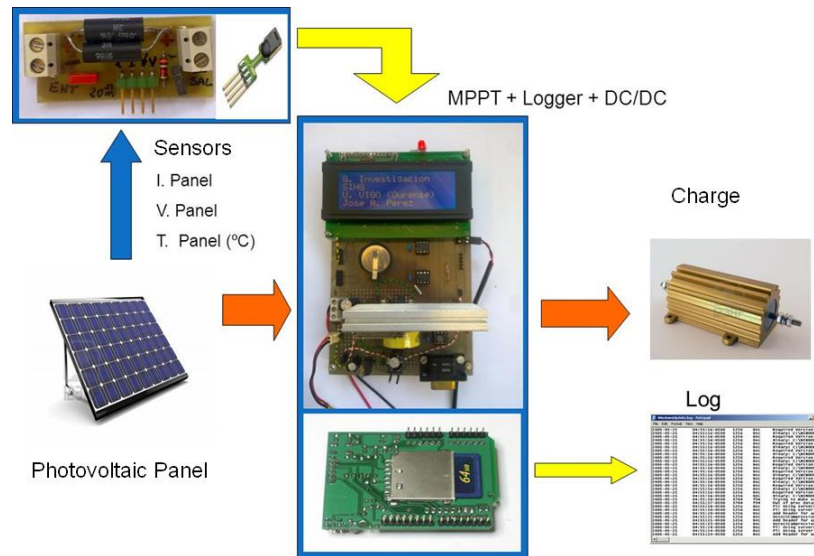


Figure 3 Data logger developed for carrying out the present work

The microcontroller will run the required software to validate MPPT by executing the Hill Climbing algorithm (developed using C programming language and a compiler for Microchip microcontrollers). Moreover, the microcontroller should also be continuously reading the external sensors and saving loaded information into a SD memory card.

The microcontroller used during the experiments belongs to the *PIC18Fxxx* family developed by Microchip [14], and includes the following features: Harvard architecture and RISC processor, clock speed up to 40 Mhz, 10-bit resolution A/D converters, 48K program flash memory, 3K RAM and 1K EEPROM memory, PWM (*Pulse-With Modulation*) 10 bits, SPI, I2C and RS232 bus communication, 3 timers and watchdog, internal and external IRQ with priority management.

The data logger requires the existence of several 10 bit resolution A/D converters [15] to continuously measure collector voltage and intensity output. We also used a temperature sensor attached to the photovoltaic collector to measure its temperature guaranteeing an error rate less than 1 °C. Moreover, the data logger contains a real-time clock to get an exact timestamp of each measurement [16]. This clock should be synchronized with the clock used by MeteoGalicia weather station located close to the collector.

During the construction of the data logger, we used a real time clock based on the chip DS1307 developed by Dallas semiconductor. This chip allows the maintenance of a real-time clock with a precision of 100 milliseconds and a maximum error rate of 5 seconds by year. Moreover, we have utilized an alphanumeric display of 4 lines and 20 characters to visualize the status of the system. Additionally, a RS232 communication interface is used to connect the data logger with the PC and a SD memory card is in charge of storing information compiled during more than one month. The data logger also contains a DC/DC

Buck-Booster converter [17] able to manage the power sent from the solar collector to load circuit. This converter is controlled from the microcontroller via PWM.

The voltage sensor is resistive and the intensity sensor was implemented using the device MAX4173 developed by MAXIM IC [18]. Finally, the temperature sensor was implemented by using the device DS1820 manufactured by Dallas semiconductor that uses one wire interface providing a precision greater than 0.5°C, and a time required for measurements lower than 700 mSeg.

■4.0 EXPERIMENTATION CARRIED OUT

Once implemented the data acquisition data logger and control system for the photovoltaic panel as described in Section 3, we carried out the motorization of real data for later preprocessing and analysis. With the goal of documenting the whole process, next subsections give details about the following aspects: (i) description of the available data sources, (ii) encountered problems and adopted solutions, (iii) data preprocessing carried out and (iv) obtained results.

4.1 Description of Available Data Sources

In order to obtain reliable, accurate and continuous environmental data we have used the service provided by MeteoGalicia (<http://www.meteogalicia.es/>), which supply the functionality of querying several atmospheric variables from its web page (e.g.: ambient temperature, relative humidity, atmospheric pressure, global solar radiation, wind velocity and direction, etc.) with a 10 minutes simple frequency [19]. Figure 4 shows a screenshot containing those available variables.

Formato dos datos

XML

Táboas de datos

Data inicial e final
[Horario UTC]

Inicial (dd/mm/yyyy) 5/4/2012 ▶

Final (dd/mm/yyyy) 6/4/2012 ▶

Tipo de Consulta

Variables dez-minutais

Variables diarias

Variables mensuais

Consultas dez-minutais: Período máximo dun mes marcando como máximo catro variables ou catro meses para unha única variable.

Ourense-Ciencias (Ourense)

	Variables dez-minutais	Altura	Data alta	Data baixa
<input type="checkbox"/>	Temperatura media do aire	1,87 m.	02/07/2005	
<input type="checkbox"/>	Humidade relativa media	1,87 m.	02/07/2005	
<input type="checkbox"/>	Temperatura de Orballo	1,87 m.	02/07/2005	
<input type="checkbox"/>	Radiación Solar Global	1,75 m.	02/07/2005	
<input type="checkbox"/>	Horas de Sol	1,75 m.	02/07/2005	
<input type="checkbox"/>	Velocidade do Vento	25 m.	02/07/2005	
<input type="checkbox"/>	Dirección do Vento	25 m.	02/07/2005	
<input type="checkbox"/>	Refacho	25 m.	02/07/2005	
<input type="checkbox"/>	Desv. típica de veloc vento	25 m.	02/07/2005	
<input type="checkbox"/>	Desv. típica de direcc vento	25 m.	02/07/2005	
<input type="checkbox"/>	Dirección do Refacho	25 m.	02/07/2005	
<input type="checkbox"/>	Chuvia	1 m.	02/07/2005	
<input type="checkbox"/>	Presión Barométrica	0,3 m.	02/07/2005	
<input type="checkbox"/>	Presión reducida ao nivel do mar	0,3 m.	02/07/2005	
<input type="checkbox"/>	Horas de luz	--	23/01/2012	
<input checked="" type="checkbox"/>	Todos			

O valor -9999 indica dato non rexistrado

Figure 4 Data acquisition functionality provided by MeteoGalicia on-line portal

Moreover, as we previously commented in Section 3, the implemented data acquisition system made possible the measurement of different variables related with the photovoltaic panel (i.e.: temperature, electric voltage and intensity).

4.2 Encountered Problems and Adopted Solutions

During the whole experimental process carried out, and taking into consideration that we have implemented both new specific hardware and firmware for the measurement of real variables, we have faced within different problems related to several issues that have been appearing.

The first problem was the implementation of the data logger and MPPT system with power converter, allowing the real time capture of measurements concerning all the variables with an appropriate precision for their later storage in a SD card. At the beginning it was intended to obtain real time measurements for (i) ambient temperature, (ii) solar radiation, (iii) temperature, electric voltage and intensity of the photovoltaic panel, (iv) wind velocity and direction, (v) atmospheric pressure, (vi) air humidity and (vii) rain fall. Once studied these analogic variables, it was concluded that it is necessary a minimum resolution of 10 bits in the A/D converter to be used in the data logger for obtaining accurate measurements [20]. Given the impossibility of having a data acquisition system with these features, we resolved to install the photovoltaic panel and the data logger in the immediate vicinity of a weather station belonging to MeteoGalicia, from which we can obtain those measurements with an appropriate sample interval and accuracy. In this way, the data logger will only store the temperature, electric voltage and intensity of the photovoltaic panel together with the exact date and hour of these measurements.

During the experimental execution, the initial weather station selected from the MeteoGalicia network (Tioira-Maceda) suffered an extensive remodeling, in which the solar radiation

sensor was suppressed on 25.january.2012. This setback compelled us to move the photovoltaic panel and the data logger to a new position (in the vicinity of the weather station Ourense-Ciencias), where all the variables were measured from 1.february.2012 to 20.april.2012.

4.3 Data Preprocessing

As a result of the monitoring and tracking process carried out from 1.february.2012 to 20.april.2012, we obtained a final log file stored by the data acquisition system in the SD card.

The stored values regarding the measurements of temperature, electric voltage and intensity of the photovoltaic panel were merged (using the exact data and hour provided by the real time clock) with those obtained from the weather station located at Ourense-Ciencias. As a result of this fusion procedure, we generated an initial file containing the measurements for all the variables which were processed as follows:

- (1) Removing of those lines containing erroneous or out of range values.
- (2) Removing of those lines with measurements from 29.march.2012 to 2.april.2012 due to a fault in the solar radiation sensor of the weather station.
- (3) Both electric voltage and intensity of the photovoltaic panel (decision variables) were merged into a unique variable (panel power= $I_{\text{panel}} \times V_{\text{panel}}$) with the goal of simplifying calculations.

Starting from the preprocessed data (containing 10652 records) and with the goal of simplifying the posterior analysis, we did not take into consideration those measurements in which the power generated by the photovoltaic panel was 0 (because we are only interested in those situations in which the photovoltaic

panel generates energy). As a result, we obtained a final file with 5102 records.

Starting from this preprocessed log file containing continuous measurements, and with the goal of applying rough sets for its analysis, we proceeded with the discretization of the variables using three, five and seven linguistic labels. The discretization procedure was carried out by using constant amplitude intervals [21].

Finally, using the obtained discretized file, we run the ROSE2 tool [22] for identifying those relevant variables using rough sets. Next subsection introduces the obtained results.

4.4 Obtained Results

For each discretized dataset, we carried out the variable reduction process by computing the discernibility matrix. In all the situations, we obtained the same six representative variables comprising the final reduct: solar radiation, temperature of the photovoltaic panel, atmospheric pressure, air humidity, ambient temperature and wind velocity. Moreover, in all the experiments we observed that rain fall was not selected as core variable for explaining the power generated by the photovoltaic panel (decision variable).

However, when computing the lower and upper approximations for the available datasets, we obtained different results for the quality of the final classification (CQ). Tables 2, 3 and 4 show the details of the experiments carried out for the three datasets, in which the quality of the final classification was computed by Equation (6), and the accuracy of each interval was calculated using Equation (7).

$$CQ = \frac{\sum_{i=1}^n \text{card}(\text{Lowerapprox}_i)}{\text{card}(U)} \times 100 \quad (6)$$

$$\text{accuracy} = \frac{\text{card}(\text{Lowerapprox})}{\text{card}(\text{Upperapprox})} \times 100 \quad (7)$$

Table 2 shows the results obtained when processing the input file containing all the variables discretized using three different intervals (low, normal and high). From the total amount of 5102 samples covering the entire Universe, 3120 belong to the low output power interval, 1824 belong to the normal power interval and 158 belong to the high power interval. A greater number of samples were obtained for the low output power interval when compared to normal and high intervals. This situation is considered reasonable because the monitoring period was winter, in which daylight hours are much lower than darkness.

Table 2 Results for the input dataset discretized using 3 intervals

Classification Quality: 69.05%				
Output Power	Samples	Lower approx.	Upper approx.	Accuracy
Low	3120	3042	4430	68.67%
Normal	1824	387	1966	19.68%
High	158	94	258	32.98%

Table 3 introduces the results obtained starting from the input file containing all the variables discretized using five different intervals (low, low-normal, normal, normal-high and high). In this case, from the total amount of 5102 samples covering the entire Universe, 2360 belong to the low output power interval, 1103 belong to the low-normal interval, 1302 belong to the normal power interval, 300 belong to the normal-high power interval and 37 belong to the high power interval.

It is interesting to highlight that the obtained accuracy for each interval does not depend on number of available samples. Regarding this issue, Table 3 shows how low and high intervals present the same accuracy (approximately 80%), but the number of samples in the low interval is 2360, significantly higher than the 37 samples belonging to the high interval.

Table 3 Results for the input dataset discretized using 5 intervals

Classification Quality: 70.11%				
Output Power	Samples	Lower approx.	Upper approx.	Accuracy
Low	2360	2300	2806	81.97%
Low-Normal	1103	558	1740	32.07%
Normal	1302	569	1580	36.01%
Normal-High	300	117	460	25.43%
High	37	33	41	80.49%

Finally, Table 4 summarizes the results obtained when processing the input file containing all the variables discretized using seven different intervals (very low, low, low-normal, normal, normal-high, high and very high). One we have presented

the obtained results from the experimentation carried out, next section details the main conclusions of the present work and outlines future research lines.

Table 4 Results for the input dataset discretized using 7 intervals

Classification Quality: 76.70%				
Output Power	Samples	Lower approx.	Upper approx.	Accuracy
Very Low	1953	1895	2204	85.98%
Low	927	616	1173	52.51%
Low-Normal	725	450	1032	43.60%
Normal	1000	625	1224	51.06%
Normal-High	413	261	560	47.86%
High	69	48	81	59.26%
Very High	15	11	17	64.71%

5.0 CONCLUSIONS

For the reasons explained in section 4.2, results of this work are based on log files generated from 1.february.2012 to 20.april.2012. In this context, it should be noted that the number of samples belonging to each interval varies significantly, as well as the environmental conditions, which reduces the scope of the study to winter conditions.

From the analysis of the obtained results (Tables 2, 3 and 4) we can conclude that the classification quality is better when using a discretization of 7 intervals for the decision variable (output power of the photovoltaic panel). Moreover, it is also observed that regardless the selected discretization (3, 5 or 7 linguistic labels), the obtained accuracy is better for the extreme labels (very low, low, high and very high).

As a final conclusion of this work, it can be stated that with the number of available samples in the monitored period, rough sets could not represent an optimal solution with regard to the reduction of physic variables governing the studied process, obtaining a global classification quality below 70% in some cases.

Future work is oriented to (i) gather new samples in different periods of time (something that we are doing now), (ii) testing new discretization algorithms (e.g.: same frequency, k-means and/or Fisher) and (iii) process all this data with rough sets variants.

Acknowledgements

The authors would like to express their sincere appreciation to both, the technical staff of MeteoGalicia for their valuable assistance, and T-Solar (<http://www.tsolar.eu/>) for the donation of the TS97 photovoltaic panel.

Appendix A: Basic operation of a photovoltaic generation system

A basic solar photovoltaic generation isolated system can be implemented as shown in Figure A.1. In this system, photovoltaic solar collectors generate energy to charge a set of batteries or power a submersible pump to extract water in isolated zones where an electric energy supply is not available.

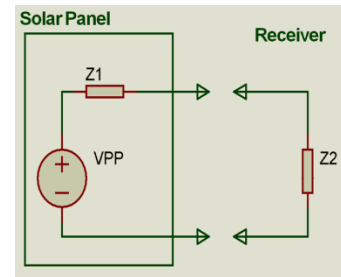


Figure A.1 Basic scheme of a photovoltaic generator

As we can see from Figure A.1, solar collector is directly connected to target or load circuit. In order to achieve an optimal system function we should keep in mind the *maximum power transfer theorem*. This theorem states that, for any energy power source or system with a constant internal impedance and voltage, we can compute the moment of maximum power transferred to load. This moment happens when impedance of load or target (batteries, submersible pumps, etc.) is equivalent to the internal impedance of source (solar collector).

$$P_{max} \Rightarrow Z_1 = Z_2$$

However, due to the load properties of solar collector and climatic environmental conditions, impedances of load and solar collector are constantly varying, generating losses of transmitted energy from collector to load from 10 and up to 35% of the whole amount of energy. In order to solve this problem, as shown in Figure A.2, we should install a MPPT system between collector and load.

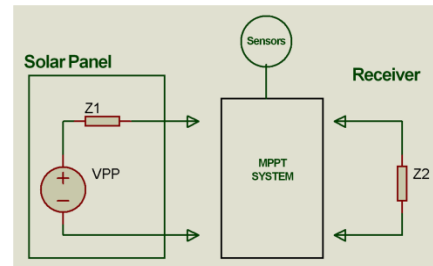


Figure A.2 MPPT system installed between load and photovoltaic collector

For clarification purposes and with the goal of illustrating this concept, Figure A.3 presents a typical 75 Watts solar photovoltaic collector curve.

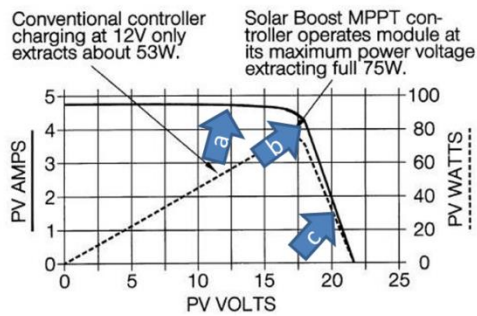


Figure A.3 Typical curve VC and photovoltaic collector power

Solid line from Figure A.3 represents VA feature of the collector that establishes the proportion between generated current and voltage as keeping into account the intrinsic features of collector and environmental conditions at any given time. In this figure, dashed line represents the power generated by collector and 'b' point establishes the maximum power point computed by MPPT system and used to improve collector function.

Appendix B: Characteristics of the photovoltaic panel donated by T-Solar (TS97 model)

The photovoltaic panel donated by T-Solar is composed by amorphous silicon single junction cells on float glass with laminated glass-glass of long term [23]. It provides an energetically effective solution under real operating conditions due to a better response to high temperatures and diffuse radiation. It is able of having a maximum rated power of 97.5 watts, with 76 volts and 1.29 amperes. The TS97 model is capable of providing the 80% of the maximum power for a period of 25 years from direct exposure to the sun.

References

- [1] Faranda R., S. Leva and V. Maugeri. 2008. MPPT Techniques for PV Systems: Energetic and Cost Comparison. Presented at the Power and Energy Society General Meeting-Conversion and Delivery of Electrical Energy in the 21st Century. 1–6.
- [2] Blaabjerg F., R. Teodorescu, M. Liserre and A.V. Timbus. 2006. Overview of Control and Grid Synchronization for Distributed Power Generation System. *IEEE Transaction on Industrial Electronics*. 53(5): 1389–1409.
- [3] Pawlak Z. 1991. *Rough Sets—Theoretical Aspects of Reasoning About Data*. Kluwer Academic Publishers.
- [4] Shuang G., D. Lei, T. Chengwei and L. Xiaozhong. 2011. Wind Power Prediction Using Time-series Analysis Base on Rough Sets. Presented at the ICEICE International Conference on Electric Information and Control Engineering. 2847–2852.
- [5] Dolara A., R. Faranda and S. Leva. 2009. Energy comparison of seven MPPT Techniques for PV Systems. *Journal of Electromagnetic Analysis and Applications*. 1(3): 152–162.
- [6] Esram T. and P.L. Chapman. 2007. Comparison of Photovoltaic Array Maximum Power Point Tracking Techniques. *IEEE Transactions on Energy Conversion*. 22(2): 439–449.
- [7] Hohm D.P. and M.E. Ropp. 2000. Comparative Study of Maximum Power Point Tracking Algorithms Using an Experimental, Programmable, Maximum Power Point Tracking Test Bed. Presented at the Photovoltaic Specialists Conference. Conference Record of the Twenty-Eighth IEEE. 1699–1702.
- [8] Ahmad J. 2010. A Fractional Open Circuit Voltage Based Maximum Power Point Tracker For Photovoltaic Arrays. 2010. Presented at the ICSTE 2nd International Conference on Software Technology and Engineering. V1-247–V1-250.
- [9] Al-Diab A. and C. Sourkounis. 2010. Variable Step Size P&O MPPT Algorithm for PV System. 2010. Presented at the OPTIM 12th International Conference on Optimization of Electrical and Electronic Equipment. 1097–1102.
- [10] Dorofte C., U. Borup and F. Blaabjerg. 2005. A Combined Two-method MPPT Control Scheme for Grid-connected Photovoltaic Systems. Presented at the EPE European Conference on Power Electronics and Applications. 10.
- [11] Jain S. and V. Agarwal. 2007. Comparison of the Performance of Maximum Power Point Tracking Schemes Applied to Single-stage grid-connected Photovoltaic Systems. *IET Electr. Power Appl.* 1(5):753–762.
- [12] Habibi M. and A. Yazdizadeh. 2009. New MPPT Controller Design for PV Arrays Using Neural Networks (Zanjan City Case Study). Presented at the ISNN 6th International Symposium on Neural Networks: Advances in Neural Networks-Part II. 1050–1058.
- [13] CADSOFT. 2011. Discover CadSoft EAGLE PCB software. <http://www.cadsoftusa.com/eagle-pcb-design-software/product-overview/?language=en>.
- [14] MICROCHIP. 2012. 8-bit PIC® Microcontrollers – Overview. <http://www.microchip.com/pagehandler/en-us/family/8bit/>.
- [15] Fernández H., A. Martínez, V. Guzmán and M.I. Giménez. 2008. A Simple, Low Cost Design Using Current Feedback to Improve the Efficiency of a MPPT-PV System for Isolated Locations. Presented at the EPE-PEMC 2008 13th Power Electronics and Motion Control Conference. 1947–1950.
- [16] Yuvarajan S. and J. Shoeb. 2008. A Fast and Accurate Maximum Power Point Tracker for PV Systems. Presented at the APEC 2008 Twenty-Third Annual IEEE Applied Power Electronics Conference and Exposition. 167–172.
- [17] Coelho R.F., F. Concer and D.C. Martins. 2009. A Study of the Basic DC-DC Converters Applied in Maximum Power Point Tracking. Presented at the COBEP '09 Brazilian Power Electronics Conference. 673–678.
- [18] MAXIM-IC. 2012. Analog, Linear, and Mixed-signal Devices from Maxim. <http://www.maxim-ic.com/>.
- [19] MeteoGalicia. 2012. Weather Stations. <http://www2.meteogalicia.es/galego/observacion/estacions/estacionsHistorico.asp?Nest=10123&prov=Ourense&tiporede=automaticas&red=102&idprov=2>.
- [20] Alippi C. and C. Galperti. 2008. An Adaptive System for Optimal Solar Energy Harvesting in Wireless Sensor Network Nodes. *IEEE Transactions on Circuits and Systems I: Regular Papers*. 55(6): 1742–1750.
- [21] ADDINSOFT. 2012. <http://www.xlstat.com/es/>.
- [22] Predki B. and S. Wilk. 1999. Rough Set Based Data Exploration Using ROSE System. Presented at the ISMIS'99 11th International Symposium on Foundations of Intelligent Systems. 172–180.
- [23] T-SOLAR. 2010. <http://www.tsolar.com/es/portal.do?IDM=282&NM=3>.